

A Contactless Power Supply for a DC Power Service

Eun-Soo Kim *and Yoon-Ho Kim **

Abstract – It is expected that, in the future, DC power service will be widely used for photovoltaic home power generation systems, since DC consuming devices are ever increasing. Instead of using multiple converters to convert DC to AC and then AC to DC, the power service could solely be based on DC. This would eliminate the need for converters, reducing the cost, complexity, and possibly increasing the efficiency. However, configuration of direct DC power service with mechanical contacts can cause spark voltage or an electric shock when the switch is turned on and off. To solve these problems, in this paper, a contactless power supply for a DC power service that can transfer electric power produced by photovoltaics to the home electric system using magnetic coupling instead of mechanical contacts has been proposed. The proposed system consists of a ZVS boost converter, a half-bridge LLC resonant converter, and a contactless transformer. This proposed contactless system eliminates the use of DC switches. To reduce the stress and loss of the boost converter switching devices, a lossless snubber with coupled inductor is applied. In this paper, a switching frequency control technique using the contactless voltage sensing circuit is also proposed and implemented for the output voltage control instead of using additional power regulators. Finally, a prototype consisted of 150W boost converter has been designed and built to demonstrate the feasibility of the proposed contactless photovoltaic DC power service. Experimental results show that 74~83% overall system efficiency is obtained for the 10W~80W load

Keywords: Contactless transformer, Resonant converter, Coupling, DC Power service

1. Introduction

Increasing demand and environmental concerns have forced engineers to focus on designing power systems with both high efficiency and green technologies. The most well-known green technologies include photovoltaics. Unfortunately, the prevailing power system infrastructures are based on AC while the photovoltaic energy produces DC. The DC output produced by photovoltaics is not directly connected to the DC consuming devices. Instead, a boost type DC/DC converter is normally used to step up the DC, then the inverter converts DC to AC to interface with power utility and this ac power is converted back to DC again to be interfaced with various DC powered home electric systems such as computers, televisions, monitors[1]-[5]. This adds complexity and reduces efficiency of the power supply system due to the need of power converters. In future, as illustrated in Fig 1(a), it is expected that the DC power service will be widely used

for a photovoltaic home power generation system, since DC consuming devices such as personal computers, vacuum cleaners, battery chargers, and various portable equipments are ever increasing. Instead of using multiple converters to convert DC to AC and then AC to DC, the power system could solely be based on DC. This would eliminate the need for converters, reducing the cost, complexity, and possibly increasing the efficiency.

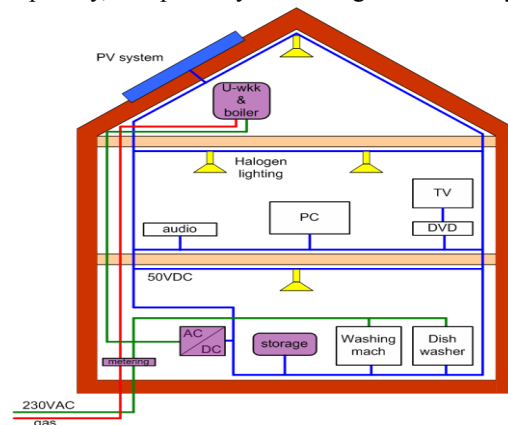


Fig. 1. DC power service using hybrid power generation system

* Dept. of Electrical & Electronics Engineering, Jeonju University, Korea. (eskim@jj.ac.kr)

** Dept. of Electrical & Electronics Engineering, Chung-Ang University, Korea. (yhkim@cau.ac.kr)

However, such configuration of the direct DC power service can cause spark voltage when the switch is turned on and off when connecting and disconnecting the load. To avoid electric shock and other problems, DC link voltage for DC power service is limited to very low voltage ($\sim 50 V_{DC}$)

To solve these problems, in this paper, a contactless power supply for a DC power service is proposed. Fig. 2 presents a proposed photovoltaic home power generation system using a contactless power supply (CPS) that can transfer an electric power without any mechanical contacts. The proposed system consists of a ZVS boost converter, a half-bridge series resonant converter, and a contactless transformer. This proposed contactless system eliminates the use of DC switches and avoids spark voltage and other problems. The proposed system steps up output voltage of the solar cell from $40\sim 60 V_{DC}$ to $84 V_{DC}$, and a contactless power supply based on a series resonant converter is used to transfer the stepped up voltage to the load safely without any influence from surrounding environments.

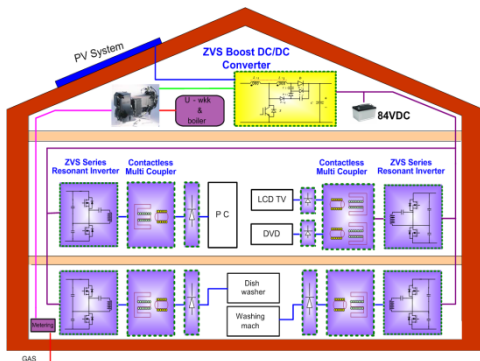


Fig. 2. The proposed DC power service using the contactless power supply

To stabilize output voltage and obtain constant output voltage, a constant output voltage controller is designed without using additional regulators. As displayed Fig 3, a separate contactless magnetic coupler to obtain output voltage signal for the output voltage controller is implemented. The control signal of the output voltage is transferred to the magnetic coupler primary side without physical contact. The transferred control signal is used to control output voltage.

To increase efficiency and reduce switching stress, soft switching techniques are applied to all the converter switching devices of the contactless power supply. Based on the theoretical analysis, the prototype of the proposed 80W DC service using a contactless power supply is

implemented to verify the proposed system. The experimental results of the prototype are then discussed.

2. The Boost Converter Based On the Lossless Snubber

To supply the boosted $84 V_{DC}$ from the solar cell output voltage ($40\sim 60 V_{DC}$) to the half-bridge inverter and a battery, a boost converter based on the high efficiency lossless snubber is designed. To reduce the switching losses of the main switching device and freewheeling diode, a coupled inductor regenerative snubber having a lossless snubber characteristic is applied to the conventional boost converter.

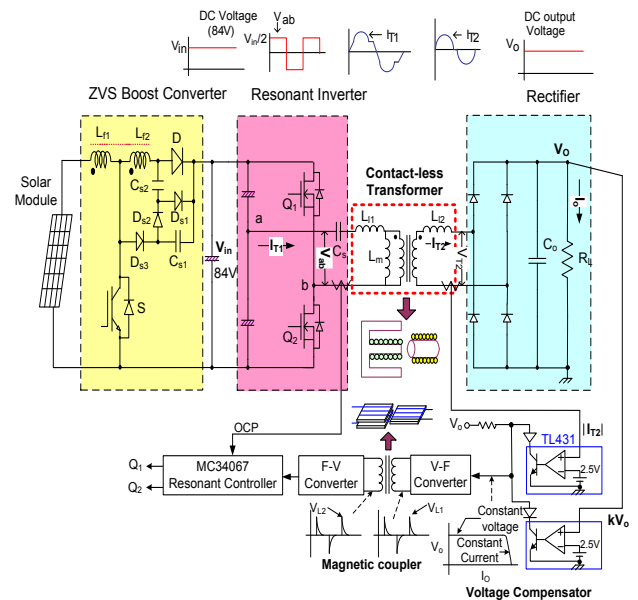


Fig. 3. Block diagram of the proposed system with output voltage controller.

Table 1. Specifications of boost converter with a lossless snubber using coupled inductor

Parameter	Value
Input voltage (V_{IN})	$40\sim 60V_{DC}$
Output voltage (V_o)	$84V_{DC}$
Output current	1.78A
Output power	150W
Switching frequency	100kHz
Primary side inductance(L_{f1})	420 μ H
Secondary side inductance(L_{f2})	15 μ H
Turn ratio (n_2/n_1) of coupled inductor	0.158(9/57)

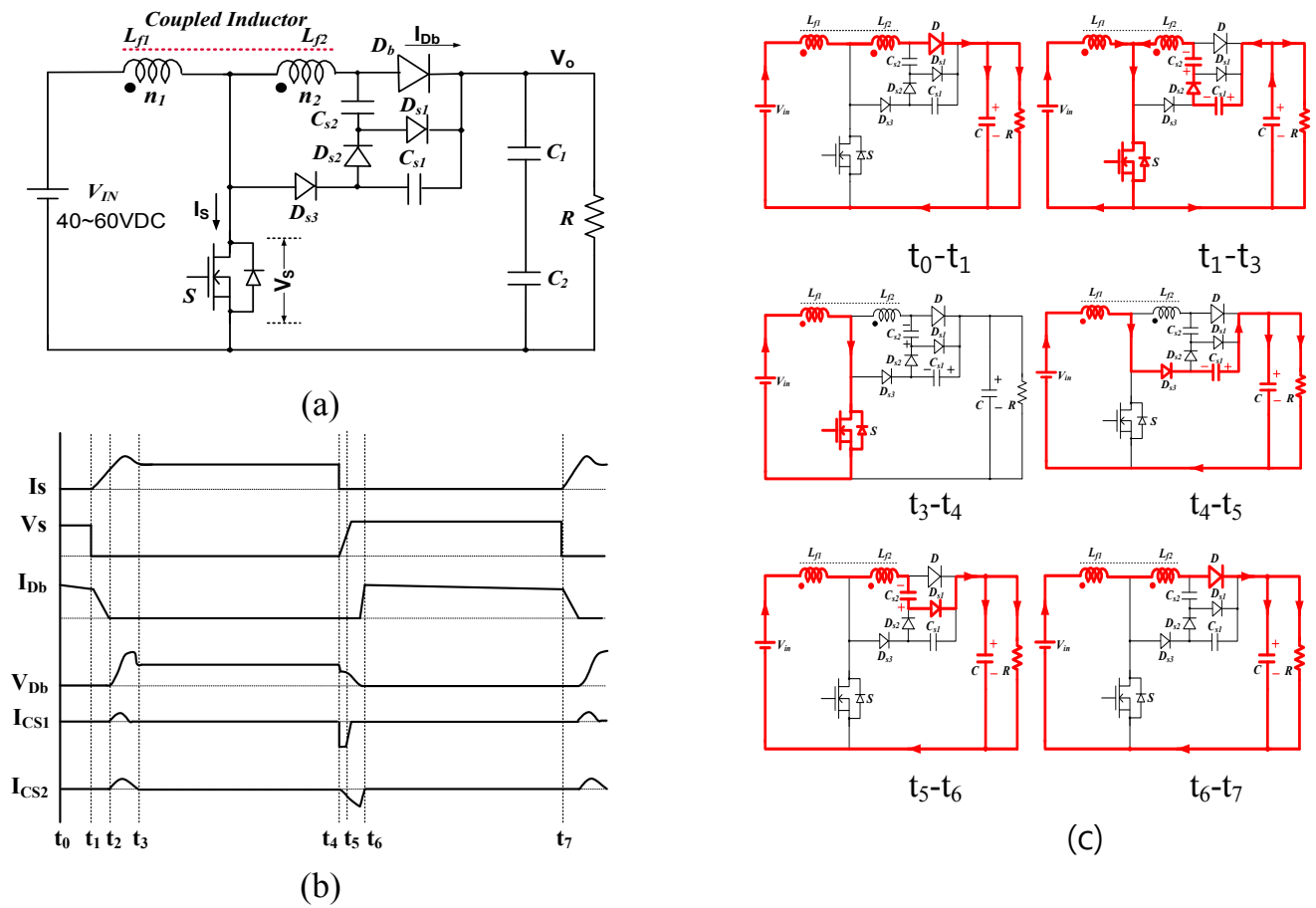


Fig. 4. The proposed high efficiency boost converter and its experimental waveforms
 (a) The proposed boost converter with lossless snubber, (b) Experimental waveforms, (c) Operating modes

Fig. 4 presents a proposed boost converter with a lossless snubber using coupled inductor and Table 1 shows parameter values of the boost converter with a lossless snubber. As shown in Fig. 4, since a low impedance path is provided by C_{s1} and C_{s2} of the snubber circuit in time period $t_1 \sim t_3$, zero voltage switching of the freewheeling diode (D_b) is achieved. Since, with the secondary leakage inductance of the coupled inductor, in turn-on period($t_1 \sim t_3$),

$$C_{s2} \text{ is charged to } V_o + \left(\frac{n_2}{n_1}\right) \cdot V_o \text{ and } C_{s1} \text{ is charged to } V_o,$$

and, in turn-off period ($t_4 \sim t_6$), as C_{s1} and C_{s2} discharges, the voltage across the main switching devices(S) is limited to the output voltage level (V_o), zero voltage switching of the main switching devices is achieved.

Also, during the interval (t_0-t_2 , t_6-t_7), since the snubber diodes D_{s1} , D_{s2} and D_{s3} are reverse biased by the secondary voltage of the coupled inductor, the coupled

3. Series Resonant Converters For The Contactless Power Transfer

Since photovoltaic output is DC, the DC power can be directly connected to the DC consuming home electric systems. However, such configuration of the direct DC power service can cause spark voltage when the switch is turned on and off for connecting and disconnecting the load. To avoid these problems, in this paper, a DC power service using a contactless power supply is proposed. A contactless power supply system based on the half-bridge series resonant converter for the DC power service as shown in Fig.3 is designed. It is assumed that multi-number of half-bridge converters can be connected with one boost converter with different power capacities.

In the contactless transformer as shown in Fig. 5, a large air-gap is made between the primary side and secondary side of the transformer. The large air-gap transformer has smaller magnetizing inductance and lower coupling

coefficient (k) than the regular transformer due to increase of primary and secondary side leakage inductance. Various applications of series resonant converters and contactless transformers such as battery chargers, artificial hearts, and electric vehicles [7]-[16] have been presented. In this paper, a high efficiency DC power service using a ZVS boost converter, a half-bridge resonant converter, and a contactless transformer is designed and implemented.

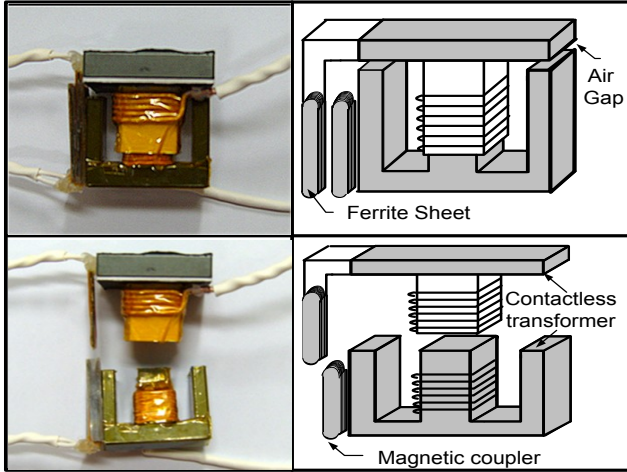


Fig. 5. Prototype of a contactless transformer for power transfer and an inductive coupler for data communication

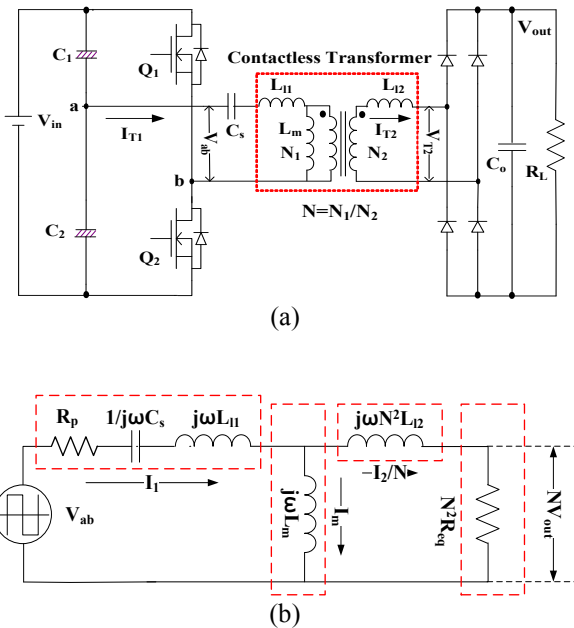


Fig. 6. Half-bridge series resonant converter using a contactless transformer (a) Half-bridge series resonant converter (b) Equivalent circuit

Fig. 6 shows a main circuit of the contactless system that consists of a half-bridge LLC resonant converter and a contactless transformer, and its equivalent circuit. V_{ab} is terminal voltage of the half-bridge converter, C_s and L_{l1} are primary side series capacitor and series leakage inductance respectively, L_m is magnetization inductance, and L_{l2} is secondary side leakage inductance. R_{eq} is an equivalent load resistance converted to the primary side. The equivalent load resistance (R_{eq}), including resistances of rectifier diodes, capacitor filters and load resistance is [17].

$$R_{eq} = \frac{8}{\pi^2} R_L \tag{1}$$

In this paper it is assumed that the winding turns-ratio ($N=N_1/N_2$) is equal to '1'. From Fig. 2(b), resonant frequency (f_r) by making equivalent load resistance (R_{eq}) short, and corner frequency (f_o) by making R_{eq} open, are obtained respectively.

$$f_r = \frac{1}{2\pi\sqrt{L_{eq} \cdot C_s}} \tag{2}$$

$$f_o = \frac{1}{2\pi\sqrt{(L_{l1} + L_m) \cdot C_s}} \tag{3}$$

When an equivalent load resistance (R_{eq}) is in short, the equivalent leakage inductance (L_{eq}) is expressed as

$$L_{eq} = \frac{L_{l1}(L_m + L_{l2}) + L_{l2}L_m}{L_{l2} + L_m} \tag{4}$$

Normalized frequency ($f_n = f_s/f_r$) is a ratio between switching frequency (f_s) and resonant frequency (f_r). 'A' is a ratio between magnetization inductance (L_m) and primary side leakage inductance (L_{l1}), 'B' is a ratio between magnetization inductance (L_m) and secondary side leakage inductance (L_{l2}), and 'Q' is a load quality factor.

$$f_n = \frac{f_s}{f_r} \tag{5}$$

$$A = L_{l1} / L_m \tag{6}$$

$$B = L_{l2} / L_m \tag{7}$$

$$Q = \frac{2\pi f_r L_{eq}}{R_{eq}} \quad (8)$$

Using equation (1) ~ (8), voltage gain (M) between input (V_{ab}) and output voltage (NV_{out}) can be expressed as

$$|M| = \left| \frac{1}{1 + A - \left(\frac{1}{f_n}\right)^2 \cdot \left(A + \frac{B}{B+1}\right) + jQ(1+B)\left(f_n - \frac{1}{f_n}\right)} \right| \quad (9)$$

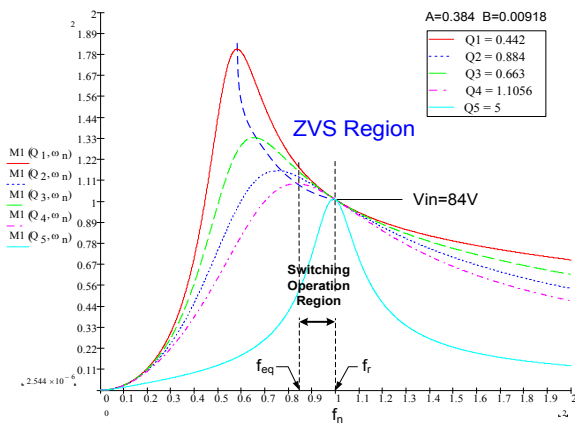


Fig. 7. Voltage gain characteristics of half-bridge series resonant converter

Fig. 7 shows voltage gain characteristics with respect to f_n and Q when the ‘A’ and ‘B’ are 0.384 and 0.00918, respectively. Fig. 7 shows the voltage gain characteristics of the proposed contactless power supply system.

It can be seen that the voltage gain of the half bridge series resonant converter increases when the normalized switching frequency is less than 1, while the gain decreases when the normalized switching frequency is greater than 1.

When the normalized switching frequency is greater than 1, the zero voltage switching (ZVS) of the main switches is obtained, but a big circulating current flows by phase difference between the primary side terminal voltage and current of the transformer.

It also has a disadvantage in that a wide range of switching frequency control is required to obtain constant output voltage for the load variation between light load and heavy load.

Moreover, it generates output voltage noises and low efficiency characteristics since ZCS operation cannot be obtained due to continuous current flow of the secondary side rectifier diode.

Table 2. Specifications of series resonant converter

Parameter	Value
Input voltage (V_{in})	84V _{DC}
Output voltage/current (V_{out}/I_o)	12V _{DC} /6.7A
Output power	80W
Switching operation region	132 kHz to 150kHz
Resonant capacitor (C_s)	0.05μF
Primary side magnetizing inductance (L_m)	51.95μH
Primary side leakage inductance (L_{l1})	19.74μH
Secondary side leakage inductance (L_{l2})	25.6nH
Equivalent leakage Inductance (L_{eq})	22.54μH
Turn ratio (N_1/N_2) of contactless transformer	3.4 (17/5)
Coupling coefficient (k)	0.828

To improve such series resonant converter problems for the contactless transformer, in this paper, switching frequency is designed to be operated in the area where the normalized resonant frequency is less than 1. In this case the zero voltage switching (ZVS) of main switches of the resonant converter is achieved and constant output voltage control can be obtained to the load variation by narrow range of switching frequency control. Moreover, since switching operation is performed in a high voltage gain area, the number of turns of the contactless transformer secondary side can be reduced. In addition, the zero current switching (ZCS) of the contactless transformers secondary side diodes is achieved due to discontinuous resonant current. Thus, the proposed contactless power supply for the DC power service has high efficiency and constant output voltage control characteristics. Table 2 presents specifications of a half bridge series resonant converter.

4. Frequency Control Using A Magnetic Coupler

The conventional contactless system obtains output voltage control signals using additional power regulators at the secondary side of the transformer. This approach reduces system efficiency and increases the system volume. In this paper, a switching frequency control technique using the contactless voltage sensing circuit is proposed for the output voltage control instead of using additional power regulators. The contactless voltage sensing circuit consists

of a magnetic coupler, v/f converter, and f/v converter as presented in Fig. 8.

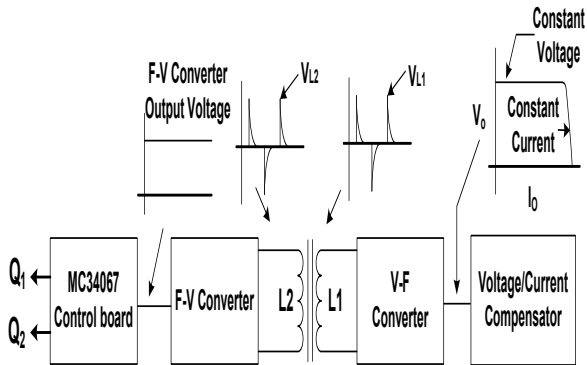


Fig. 8. Contactless voltage sensing circuit using magnetic coupler.

An output voltage signal is detected at the output side and an error signal is made by comparing with a reference signal. The error signal is converted to the ac signal by the v/f converter and the converted signal is transferred by the magnetic coupler. Then the transferred signal is converted back to the dc signal by the f/v converter and the final DC signal is used to control the output voltage by controlling the switching frequency at the main system controller.

However, since the magnetic coupler used for the data transfer has a very low coupling coefficient due to its large leakage inductance and low magnetizing inductance, this may cause some problems in transferring signals from the primary side to the secondary side of the coupler.

Table 3. Specifications of a magnetic coupler used for the data transfer

Parameter	Value
Primary side magnetizing inductance	16.83μH
Secondary side leakage inductance	24.42μH
Primary side leakage inductance	57.16μH
Coupling coefficient	0.113

Therefore, a winding design technique such that the primary side control signals of the coupler are transferred without being affected by the magnetic flux of the main transformer is proposed. As presented in Fig. 5(c) and (d), the primary side of the proposed magnetic coupler has a shape ‘—’ while the secondary side has a shape ‘⊔’ or

‘—’ and the winding direction between the contactless transformer and magnetic coupler is designed to be at a right angle to minimize the effect of the magnetic flux of the contactless transformer to the magnetic coupler.

Fig. 5 shows the newly designed magnetic coupler, and the specification of the magnetic coupler for the data transfer is given in table 3.

5. Experimental Results

In this paper, an 80W half-bridge resonant converter with a contactless transformer and a 150W boost converter with lossless snubbers is designed and implemented. The boost converter steps up the solar cell output DC voltage from low voltage (40~60 V_{DC}) to high voltage (84 V_{DC}). Table 4 describes components used in the boost converter and half-bridge series resonant converter. The specifications of the solar cell module are given in Table 5.

Table 4. Components used in a boost converter and a half-bridge series resonant converter

Boost converter with lossless snubber using coupled inductor	
Switching device (S)	IRFP250N, 200V, 30A
Freewheeling diode (D)	20CTH03, 300V, 20A
Snubber diode (D _{s1} , D _{s2} , D _{s3})	UF5402, 200V, 3A
Snubber capacitor (C _{s1} , C _{s2})	4.7nF (C _{s1}) 11nF (C _{s2})
Half-bridge series resonant converter using contactless transformer	
Switching device (Q ₁ , Q ₂)	IRF640, 200V, 18A
Input capacitor (C ₁ , C ₂)	6800uF, 50WV
Output rectifying diode	STPS1545D, 45V, 15A

Table 5. Specifications of solar cell module

Solar cell Module (SE-M181×2)	
Output capacity	362W(181W×2)
Max output voltage	53.8V _{DC}
Max output current	6.73A

The experimental waveforms of the terminal voltage and current of the main switching device (Fig. 9) display that the freewheeling diode (D_b) achieves ZVS turn-on and turn-off through low impedance path of C_{s1} and C_{s2}, while the

main switch(S) achieves ZVS turn-off through discharge of the snubber capacitors (C_{s1}, C_{s2}).

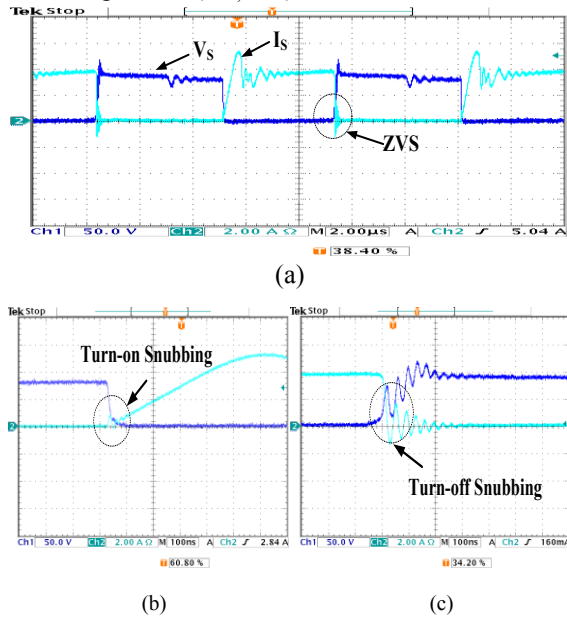


Fig. 9. Experimental waveforms of terminal voltage (V_s) and current (I_s) in a main switching device (S) when load condition is 150W. (a) [50V/div.,5A/div.,1 μ s/div.], (b), (c) [50V/div.,5A/div.,100ns/div.]

The experimental waveforms of the primary side voltage current and the secondary side current of the contactless transformer (Fig. 10) indicate that the system operates with lower switching frequency than the resonant frequency; the main switching devices (Q_1, Q_2) achieves ZVS switching while the terminal current (I_{T1}) is always lagging to the terminal voltage; and the ZCS operation of rectifier diodes is achieved due to discontinuous current (I_{T2}).

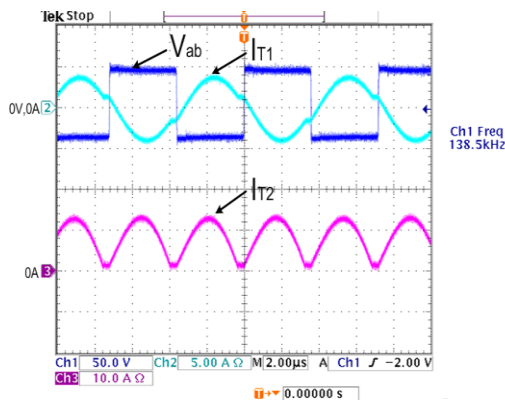


Fig. 10. Experimental waveforms of the primary voltage (V_{ab}) and current (I_{T1}), and the secondary current (I_{T2}) with 80W load

Fig. 11 displays voltage waveforms of the primary and secondary side of a magnetic coupler for data communication. The primary side waveform (Fig. 11) is an output of the v-f converter. Although the signal is reduced by the coupler due to the low coupling coefficient, the output voltage control signal (error signal) was successfully obtained by using the f-v converter. Fig. 12 displays experimental output voltage (V_o) and output current (I_o) waveforms in terms of load variations. It can be seen that even when load changes for 12W to 80W and from 80W to 7.2W, the output voltage is controlled to be constant.

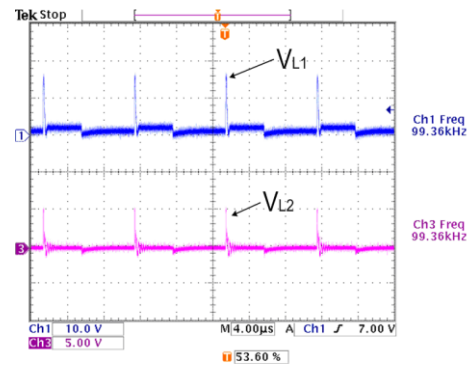


Fig. 11. Voltage waveforms of the primary and secondary in a magnetic couple for data communication

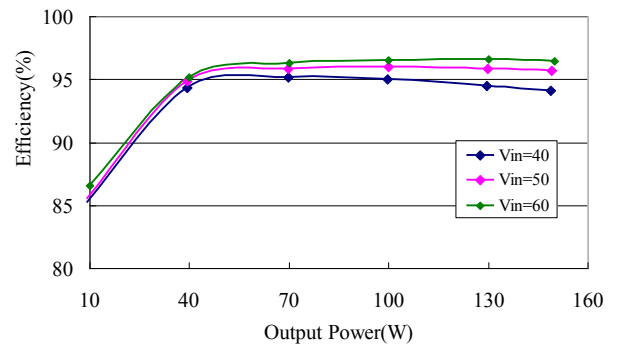


Fig. 12. The efficiency characteristics of the boost converter

The efficiency characteristics of the boost converter having a lossless snubber to the input voltage and load variation can be observed in Fig. 12. The efficiency is measured for the load variation (10W ~ 150W) and input voltage variation (40~60V_{DC}), considering that the solar cell output voltage varies by the amount of sun light. The 86~96.6% efficiency was obtained.

Fig. 13 shows the efficiency characteristics of half bridge resonant converter in the conditions of the load variation (10W ~ 80W) and input voltage (84V_{DC}). The 81~87% efficiency was obtained because of the use of bridge rectifier as shown in Fig. 6.

Fig.14 presents efficiency characteristics of the overall system to the load variation. The 74~83% efficiency was obtained to 10W~80W load when the input voltage (V_{IN}) of the boost converter varies with 40~60V_{DC}. Fig. 16 displays a photograph of the LCD TV successfully operated by the developed DC power service based on the contactless power supply

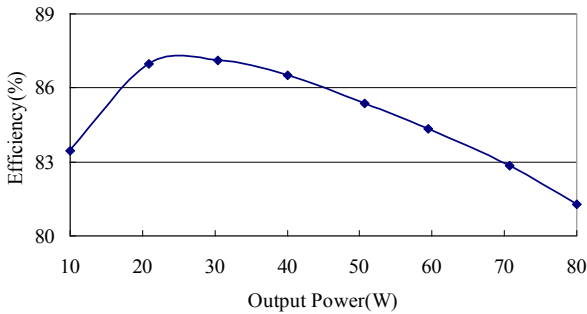


Fig.13. Efficiency characteristics of half-bridge series resonant converter

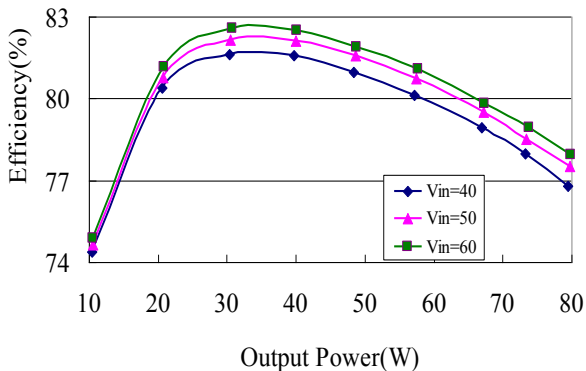


Fig. 14. Efficiency characteristics of the contactless power supply including a boost converter , a half-bridge series resonant converter, and a contactless transformer



Fig. 15. Prototype of a contact-less power supply for the photovoltaic power generation system LCD TV

6. Conclusion

In this paper, a DC power service using a contactless power supply that can transfer electric power to the home electric system without any mechanical contact by using magnetic coupling instead of power transfer with mechanical contact has been proposed. To reduce the stress and loss of the boost converter switching devices, lossless snubber with coupled inductor has been designed. A switching frequency control technique using the contactless voltage sensing circuit instead of using additional power regulators has also been proposed and successfully implemented for the output voltage control.

The experimental DC power service system using an 80W half-bridge resonant converter, a contactless transformer, and a 150W boost converter with lossless snubbers has been designed and implemented to investigate the feasibility of the DC power service based on a contactless power supply. Experimental results has shown that 74~83% overall system efficiency was obtained with 10W~80W load. The LCD TV was successfully operated by the developed DC power service based on the contactless power supply. Since the proposed system transfers DC power without mechanical contacts, it does not need mechanical on/off DC switch and avoids surge and spark voltage. The prototype has demonstrated the possibility that the contactless system can be applied to the DC power service

References

- [1] Gurkaynak, Y., Khaligh, A., “Control and Power Management of a Grid Connected Residential Photovoltaic System with Plug-in Hybrid Electric Vehicle (PHEV) Load” Applied Power Electronics Conference and Exposition, 2009. APEC 2009. Twenty-Fourth Annual IEEE
- [2] Bangyin Liu, Chaohui Liang, Shanxu Duan; “Design Considerations and Topology Selection for DC Module Based Building Integrated Photovoltaic System” Industrial Electronics and Applications, 2008. ICIEA 2008. 3rd IEEE Conference on 3-5 June 2008 Page(s):1066 – 1070
- [3] Rodriguez-Otero, M.A.; O'Neill-Carrillo, E.; “Efficient Home Appliances for a Future DC Residence” Energy 2030 Conference, 2008. ENERGY 2008. IEEE 17-18 Nov. 2008 Page(s):1 – 6
- [4] Engelen, K., Leung Shun, E.; Vermeyen, P., Pardon, I., D'hulst, R., Driesen, J., Belmans, R., “The Feasibility of Small-Scale Residential DC Distribution Systems” IEEE Industrial Electronics, IECON 2006 - 32nd Annual Conference on 6-10 Nov. 2006 Page(s):2618 – 2623
- [5] Browne, T. J., Browne, N. R., “Power Quality Considerations for Utilities Supplying Residential DC Installations” Harmonics and Quality of Power, 2008. ICHQP 2008. 13th International Conference on Sept. 28 2008-Oct. 1 2008 Page(s):1 – 5

- [6] Bangyin Liu, Shanxu Duan, Yong Kang, "A DC-Module-Based Power Configuration for Residential Photovoltaic Power Application" Power Electronics and Drive Systems, 2007. PEDS '07. 7th International Conference on 27-30 Nov. 2007 Page(s):631 - 636
- [7] G. Joung, B. Cho, "An Energy Transmission System for an Artificial Heart Using Leakage Inductance Compensation of Transcutaneous Transformer." IEEE Transactions on Power Electronics 1998, 13(6):1013-1022.
- [8] T. Nishimura, K. Hirachi, Y. Maejima Y, K. Kuwana K, M. Saito, "Characteristics of a Novel Energy Transmission for a Rechargeable Cardiac Pacemaker by Using a Resonant DC-DC converter." IEEE IECON'93 1993; 2:875-880.
- [9] J. De Boeij, E. Lomonova, and A. Vandenput, "Contactless Energy Transfer to a Moving Load - Part I : Topology Synthesis and FEM simulation," IEEE International Industrial Electronics, Page(s): 739-744, July 2006
- [10] C. Wang, G.A. Covic, O.H. Stielau, Power Transfer Capability and Bifurcation Phenomena of Loosely Coupled Inductive Power Transfer Systems, IEEE Trans. On Industrial Electronics, Vol.51, NO. 1, Feb.2004, pp. 148-157
- [11] K.D. Papastergiou, D.E. Macpherson, "An Airborne Radar Power Supply with Contactless Transfer of Energy - Part I: Rotating Transformer," IEEE Trans. Ind. Electronics, Vol. 54, NO. 5, pp 2874 – 2884, Oct. 2007
- [12] L. Xun; S.Y. Hui: "Simulation Study and Experimental Verification of a Universal Contactless Battery Charging Platform With Localized Charging Features," IEEE Trans. Power Electronics, Vol. 22, NO. 6, Page(s): 2202-2210, Nov.2007
- [13] X. Kiu; S.Y.R. Hui: "Optimal Design of a Hybrid Winding Structure for Planar Contactless Battery Charging Platform", IEEE Trans. Power Electronics, Vol. 23, No. 1, Page(s):455-463, Jan.2006
- [14] K.D. Papastergiou, D.E. Macpherson; F. Fisger, "An Airborne Radar Power Supply with Contact-less Transfer of Energy – Part I: Rotating transformer," IEEE Trans. Ind. Electronics, Vol. 54, no. 5, pp. 2874-2884, Oct 2007
- [15] M.G. Egan, D.L. O'Sullivan, J.G. Hayes, M.J. Willers, and C.P. Henze, "Power-Factor-Corrected Single-Stage Inductive Charger for Electric Vehicle Batteries," IEEE Trans. Ind. Electronics Vol. 54, no.2, pp. 1217-1226, April 2007
- [16] P. Sergeant, and A. Van den Bossche, "Inductive Coupler for Contactless Power Transmission," IET Electric Power Applications, Vol. 2, no. 1, pp.1-7, Jan. 2008
- [17] R. Steigerward, "A comparison of Half-bridge Resonant Converter Topologies". IEEE Transactions on Power Electronics, 1988; 3(2):174-182.. 4



Eun-Soo Kim received the B.S., M.S. and Ph.D degrees from Chung-Ang University, Seoul, Korea in 1986, 1988 and 2000 respectively.

From 1989 to 2001, Dr. Kim was a senior researcher and technical leader at Power Electronics Research Division in Korea Electrotechnology Research Institute (KERI).

Since 2001, He is currently a Professor in the Department of Electric & Electronics Engineering, Jeonju University, Korea. His primary areas of research interest include soft switching dc/dc converters, PDP/LCD/LED TV display power supplies, and contact-less power supply.

Dr. Kim is a committee member of Korea Institute of Power Electronics (KIPE) and the Korea Institute of Electrical Engineers (KIEE).



Yoon-Ho Kim received the B.S. degree from Seoul National University, Seoul, Korea, the M.S. degree from the State University of New York, Buffalo, and Ph.D. degree from Texas A&M University, College Station, all in electrical engineering.

He is currently a Professor in the Department of Electric & Electronics Engineering, Chung-Ang University, Seoul, Korea. His main interests are industrial electronics and drives.

Dr. Kim was a President of the Korean Institute of Power Electronics in 2003. Also, Dr. Kim was a President of the Korean Society for Railway from 2008 to 2009.